Gap and dark solitons in discrete photorefractive media with intensity-resonant nonlinearity

M. Stepić · A. Maluckov · D. Kip

Abstract Light propagation in one-dimensional nonlinear waveguide arrays with self-defocusing intensity-resonant nonlinearity is investigated theoretically. We study thoroughly conditions for existence and stability of both gap and discrete dark solitons. According to the linear stability analysis both fundamental types (on-site and intersite) of gap solitons may be stable. Discrete dark solitons are unstable except in the low-power regime and, depending on system parameters, evolve into either gray solitons, breathers, or background radiation. Mobility of these solitons is analyzed by the free energy concept: gap solitons are immobile but dark solitons can be easily set in motion.

PACS 42.65.-k · 42.65.Tg · 42.65.Wi

1 Introduction

The discovery of photorefractive solitons represents an important turning point in history of spatial solitons' investigations [1–4]. Theoretically, novel non-Schrödinger models emerged and are now used to describe soliton formation

M. Stepić (✉)
Vinča Institute of Nuclear Sciences, P.O. Box 522,
11001 Belgrade, Serbia
e-mail: mstepic@vinca.rs

A. Maluckov
Faculty of Sciences and Mathematics, University of Niš,
18000 Niš, Serbia

D. Kip
Institute of Physics and Physical Technologies, Clausthal
University of Technology, 38678 Clausthal-Zellerfeld, Germany

under a variety of photorefractive nonlinear effects. Experimentally, spatial solitons were directly visualized for the first time. Remarkably, photorefractive solitons exist at microwatt and lower power levels, while their formation time ranges from microseconds to minutes. Thus, these solitons may be observed in fairly cheap and simple optical setups.

Photorefractive lattice solitons form a specific subgroup of spatial photorefractive solitons [5]. They are observable in systems in which the refractive index periodically changes on the scale of the wavelength of the used light, for example in uniform one-dimensional (1D) and two-dimensional nonlinear waveguide arrays (NWAs) [6, 7].

Indium phosphide doped with iron (InP:Fe) exhibits a resonant enhancement of both light-induced space–charge fields and two-wave mixing gain, with a measured microsecond response at microwatt power level and telecommunication wavelengths [8, 9]. Spatial soliton formation in the bulk was recently explored in this photorefractive material [10, 11]. In [12], existence, stability, and mobility of bright discrete intensity-resonant solitons have been studied in detail [13].

The aim of this article is to investigate which solitons may be found in 1D NWAs with intensity-resonant self-defocusing nonlinearity and which features they have. The article is organized as follows: A theoretical model for light propagation in such media is given in Sect. 2. Section 3 is devoted to existing stationary solutions whose stability and mobility are explored in Sects. 4 and 5, respectively. Future prospects and a summary conclude the article in Sect. 6.

2 General treatment

Nonlinear optical-wave propagation within the first band of an arbitrary periodic structure may be fairly well described

by a discrete model based on the coupled mode approach [13, 14]. Our model equation can be reduced to the following set of dimensionless ordinary differential equations [12, 15]:

$$i\frac{dU_n}{d\xi} + U_{n+1} + U_{n-1} - 2U_n + \gamma\frac{U_n}{1-|U_n|^2} = 0, \qquad (1)$$

in which U_n is the normalized amplitude of the electrical field in the n-th element of the NWA, $\xi = z/kx_0^2$ is the normalized propagation coordinate, and $\gamma < 0$ is a normalized nonlinear coefficient. An arbitrary scaling factor in transverse direction is denoted with x_0, wave number $k = 2\pi n_0 \lambda_0^{-1}$ whereas n_0 is the refractive index of the light in the substrate and λ_0 represents the wavelength of light in vacuum. In this model, resonance occurs for $I = |U_n|^2 = 1$.

There are only two integrals of motion: power $P = \sum |U_n|^2$ and Hamiltonian $H = \sum[|U_{n-1} - U_n|^2 + \gamma \ln(1 - |U_n|^2)]$, thus the system is not integrable in the general case. In what follows we use values from [11] which give us $|\gamma| \propto 1$.

The model equation (1) maps onto itself under the transformation $U_n = V_n^*(-1)^n \exp(-4i\xi)$ and $\gamma \to -\gamma$ [16]. Therefore, considerations for the self-defocusing nonlinear lattice can be related to the case of the self-focusing nonlinearity [12].

3 Classification of solutions

The simplest solution of our model equation is a plane-wave solution of form $U_n = U_0 e^{(iKn - i\omega\xi)}$ with $K = 0$ for the unstaggered case (adjacent elements are in-phase) and $K = \pi$ for the staggered case (adjacent elements are out-of-phase). In the staggered case, the plane-wave amplitude reads: $U_0 = \sqrt{(4 - \omega - \gamma)/(4 - \omega)}$ whereas $\omega \notin (4, 4 - \gamma)$. According to the literature [16], in the presence of a self-defocusing (DF) nonlinearity, plane-wave staggered solutions are modulationally unstable, which allows for the formation of staggered bright solitons, while unstaggered solutions are stable providing a stable background for the creation of unstaggered dark solitons. On the other hand, in the self-focusing (SF) case unstaggered plane waves are modulationally unstable, which gives rise to unstaggered bright solitons [12], while the corresponding staggered solutions are stable, thus supporting staggered dark solitons. Because here the topic is a self-defocusing nonlinear lattice, staggered bright solitons and unstaggered dark solitons are investigated. The results for staggered dark solitons in SF nonlinear lattices are qualitatively the same due to the symmetry between SF and DF nonlinear lattices.

Kivshar suggested that bright staggered localized modes may be found in discrete systems provided that anomalous diffraction exactly counteracts self-defocusing nonlinearity [14]. Such modes, whose propagation constants are

pushed by nonlinear effects into the gaps of the linear structure, are also known as gap or Bragg solitons [17–19].

The discrete distribution of symmetric ($U_n = F_n e^{iKn - i\omega\xi}$, $F_n = F_{-n}, n \in [-N/2, N/2], |F_{n_c}| \gg |F_{n_c \pm 1}| \gg \cdots \gg |F_{n_c \pm N/2}|$) on-site (os) mode amplitudes is readily obtained from (1):

$$F_{\text{os}} \equiv F(n_c = 0) = \sqrt{\frac{2 - \omega - \gamma}{2 - \omega}}, \qquad F_m = \eta^m F_{\text{os}}, \qquad (2)$$

where n_c denotes the central channel of the NWA, $m \in [1, N/2]$ and $\eta = (\omega - 2 + \gamma)^{-1}$. Such solutions may exist provided that $\omega \notin (2, 2 - \gamma)$.

For the symmetric intersite (is) mode, we find:

$$F_{\text{is}} \equiv F(n_c = \pm 1) = \sqrt{\frac{1 - \omega - \gamma}{1 - \omega}}, \qquad F_{\pm m} = \eta^{m-1} F_{\text{is}}, \qquad (3)$$

where $F(n_c = \pm 1)$ symbolically presents a symmetric intersite mode centered between two neighboring lattice elements indexed as -1 and 1, η is defined as before while $m \in [1, N/2]$. These intersite solutions are forbidden only in $\omega \in (1, 1 - \gamma)$.

Dark solitons represent intensity dips on an otherwise stable uniform background, where the phase has a π jump in the center of the structure [20–22]. We focus our attention on two fundamental discrete dark solitons: on-site solitons, given by $(\ldots, 1, 1, 1, 0, -1, -1, -1, \ldots)$ and intersite ones, which have the following amplitude pattern $(\ldots, 1, 1, 1, -1, -1, -1, \ldots)$, see Fig. 2 of [22].

Stationary soliton configurations are numerically obtained by a modified Pauell minimization method, and the evolution difference-differential equations (1) are solved by a sixth-order Runge–Kutta numerical procedure [12, 16]. In all simulations periodic boundary conditions are used.

4 Stability considerations

4.1 Stability of uniform solutions

The phenomenon of discrete modulational instability, which represents a plane-wave disintegration under combined effects of diffraction and nonlinearity, is responsible for soliton formation in NWAs [13, 14, 23, 24].

We insert a perturbed solution $[U_0 e^{iKn} + \delta U_n(\xi)e^{i\kappa n}] \times e^{-i\omega\xi}$ into (1), where $|\delta U_n| \ll U_0$, and $\kappa = 0$ and $\kappa = \pi$ denote unstaggered and staggered perturbations, respectively, and obtain the following difference-differential equations for small perturbations:

$$i\frac{d\delta U_n}{d\xi} + \cos\kappa(\delta U_{n+1} + \delta U_{n-1}) - 2\cos(K)\delta U_n$$

$$+ \gamma\frac{U_0^2}{(1 - U_0^2)^2}(\delta U_n + \delta U_n^*) = 0. \qquad (4)$$

By adopting the complex perturbation form from [13]:
$\delta U_n = \epsilon_1 \exp[i(Q\xi - n\Omega\Lambda)] + \epsilon_2 \exp[-i(Q\xi - n\Omega\Lambda)]$,
in which $\epsilon_{1,2}$ are the constants, Λ is the period of NWA while Q and Ω are the parameters of a modulated wave, we obtain the following dispersion relation:

$$Q^2 = 4[\cos K - \cos(\Omega\Lambda)\cos\kappa]$$
$$\times \left[\cos K - \cos(\Omega\Lambda)\cos\kappa - \gamma \frac{U_0^2}{(1-U_0^2)^2}\right]. \quad (5)$$

Instability occurs when $Q^2 < 0$, from which one may deduce that the modulationally unstable region is bounded from both below and above:

$$1 + \frac{\gamma}{2\alpha}\left[1 - \sqrt{1 + \frac{4\alpha}{\gamma}}\right] < U_0^2 < 1 + \frac{\gamma}{2\alpha}\left[1 + \sqrt{1 + \frac{4\alpha}{\gamma}}\right], \quad (6)$$

where $\alpha = \cos K - \cos(\Omega\Lambda)\cos\kappa$.

4.2 Stability of gap solitons

There are different approaches to study the stability of gap solitons [25, 26]. We employ the linear stability analysis [27] in which fundamental soliton solutions are slightly perturbed $U_n = (F_n e^{iKn} + \delta U_n e^{i\kappa n})e^{-i\omega\xi}$, where $\delta U_n = a_n + ib_n$ is complex and $a_n, b_n \propto e^{\lambda\xi}$. After cumbersome but straightforward procedure we get the following eigenvalue problem:

$$\lambda \begin{pmatrix} a_n \\ b_n \end{pmatrix} = \begin{bmatrix} 0 & H^+ \\ -H^- & 0 \end{bmatrix} \begin{pmatrix} a_n \\ b_n \end{pmatrix} \equiv \mathbf{M} \begin{pmatrix} a_n \\ b_n \end{pmatrix}, \quad (7)$$

where the matrix $\mathbf{M}$ (of size $2N \times 2N$ for the NWA with N sites) is, generally, non-Hermitian. Elements of submatrices $H^\pm$ are

$$H_{jk}^+ = \left[-(\omega - 2) - \frac{\gamma}{1 - F_j^2}\right]\delta_{jk} - \cos\kappa(\delta_{j,k+1} + \delta_{j,k-1}),$$

$$H_{jk}^- = H_{jk}^+ - \gamma \frac{2F_j^2}{(1 - F_j^2)^2}\delta_{jk}, \quad (8)$$
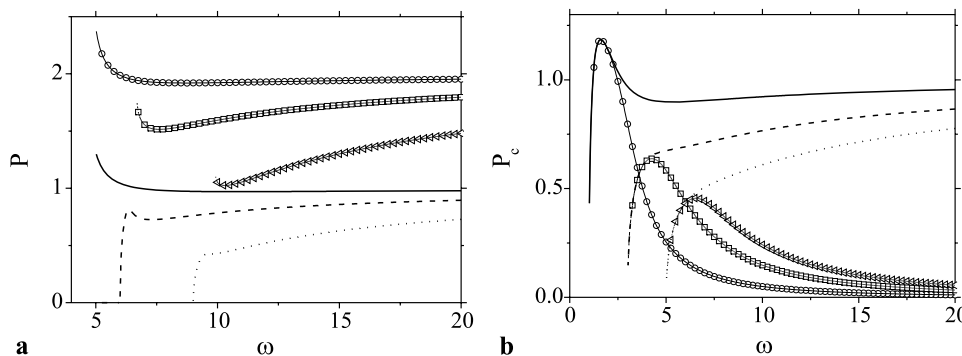
where δ_{ij} are Kronecker deltas.

From Fig. 1a, in which is given the dependence of power on propagation parameter ω for on-site staggered gap solitons and intersite staggered bright solitons, one can conclude that intersite modes always have a higher power than the corresponding on-site modes with the same ω. Furthermore, it is possible to find two different fundamental on-site solitons for a given power value in the region $\gamma < -1$.

We apply the eigenvalue spectral analysis to determine the soliton stability. Pairs of open circles in Figs. 2a, 2b indicate the onset of exponential instability only for small values of parameter ω. For higher values of parameter ω, both (marginally) stable on-site and intersite gap solitons exist. An example of stable propagation of an intersite mode with $P = 1.831$, $\gamma = -2$, and $\omega = 11.3$ is given in Fig. 3a. Diffraction of an on-site staggered mode under transverse perturbation with $\gamma = -2$, $P = 0.917$, and $\omega = 11.375$ is shown in Fig. 3b.

4.3 Stability of discrete dark solitons

We conclude this Section by studying the stability of dark solitons [28–30]. Here we follow the procedure outlined in [16], in which it was demonstrated that both on-site and intersite dark solitons may be marginally stable in 1D lattices with saturable nonlinearity. For both dark modes instability occurs in almost the whole parameter space, see Figs. 2c and 2d. While the on-site configuration develops oscillatory instability associated with two pairs of complex eigenvalues


Fig. 1 (a) Dependence of power on propagation parameter ω for on-site staggered gap solitons and intersite staggered bright solitons. The values of the nonlinearity parameter are $\gamma = -0.5$ (*solid line*), $\gamma = -2$ (*dashed line*), and $\gamma = -5$ (*dotted line*). The corresponding intersite modes are denoted as: *solid line with circles*, *dashed line with squares*, and *dotted line with triangles*, respectively. (**b**) The same dependence and notation for on-site unstaggered dark solitons and intersite unstaggered dark solitons. Here $\gamma = -1, -3, -5$, respectively

Fig. 2 Eigenvalues spectrum for (**a**) on-site staggered gap soliton, (**b**) intersite gap soliton, (**c**) on-site unstaggered dark soliton, and (**d**) intersite unstaggered dark soliton. Nonlinearity parameter for both gap and dark solitons is $\gamma = -1$. *Open circles* denote pure real eigenvalues, *full circles* depict real part of complex eigenvalues, *open squares* represent imaginary part of complex eigenvalues, whereas extremal pure imaginary eigenvalues are marked with *dashed lines*
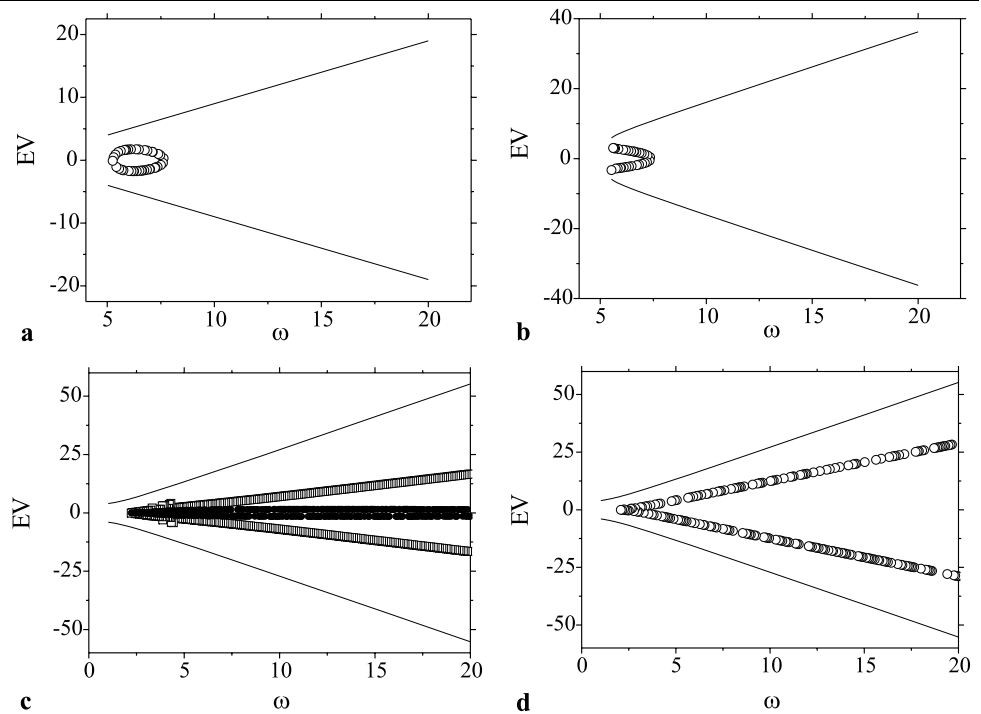

Fig. 3 (**a**) Stable propagation of intersite staggered mode with $P = 1.831$, $\gamma = -2$, and $\omega = 11.3$. (**b**) Diffraction of the on-site staggered soliton in the presence of a small transversal perturbation. Here $\gamma = 2$, $P = 0.917$, $\omega = 11.375$. (**c**) Transition of dark into gray discrete soliton for $\gamma = -3$, $\omega = 3.525$. (**d**) Disintegration of transversally perturbed dark on-site soliton having $\gamma = -3$, and $\omega = 5$ (*top view*)
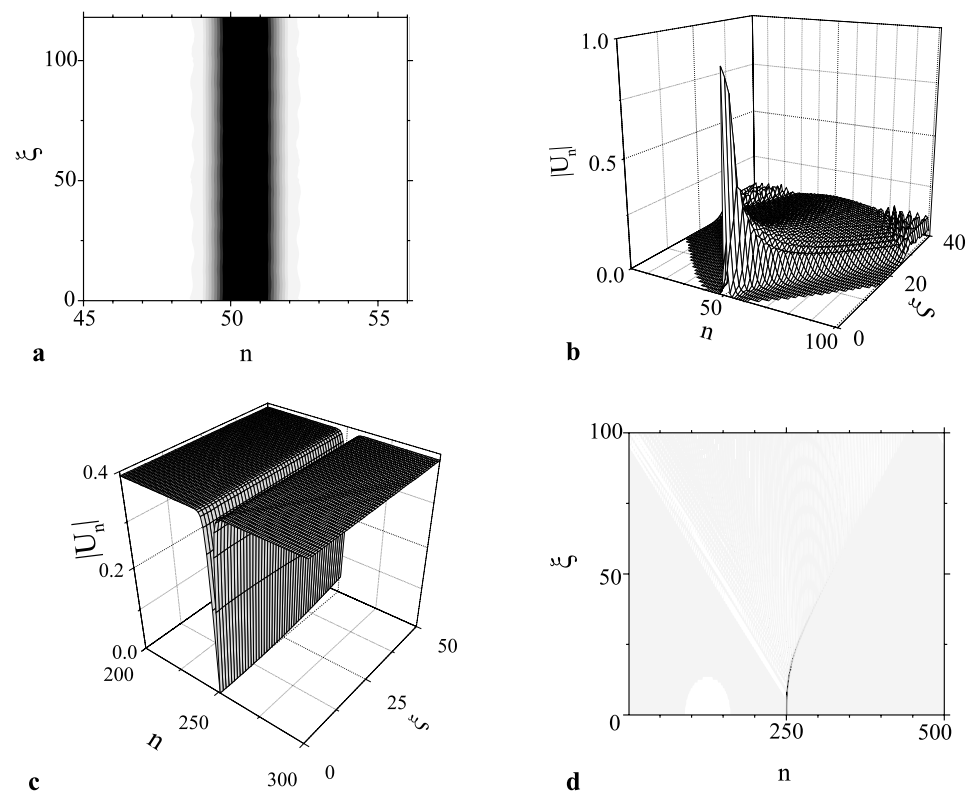

with nonzero real part in Fig. 2c, the intersite dark configuration develops an exponential instability which is associated with two pure real eigenvalues in Fig. 2d. However, for small values of propagation parameter ω, marginal stability of both kind of solitons is possible. We note the existence of

two branches of on-site dark solitons with the same power and different propagation constant, see also Fig. 1b. Here only the one with smaller value ω, which has a close intersite counterpart with the same power, is marginally stable. Unstable discrete dark solitons may evolve in stable gray
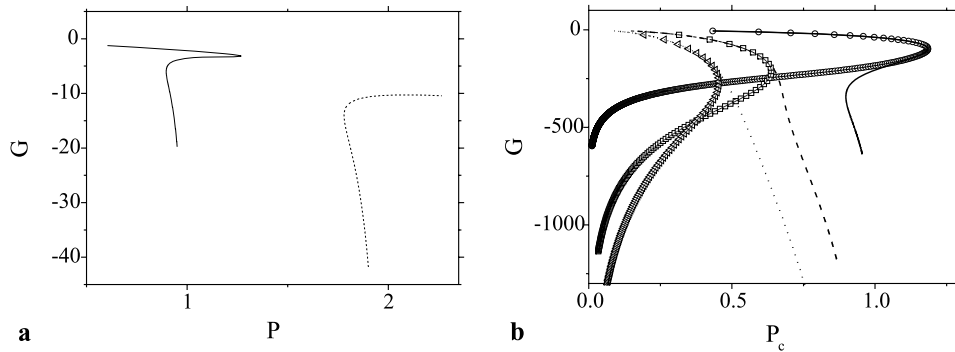
Fig. 4 Dependence of free energy G on propagation parameter ω for (**a**) gap solitons and (**b**) dark unstaggered solitons. In (**a**), $\gamma = -1$, on-site soliton is denoted with *solid line* whereas intersite soliton is denoted with *dashed line*. Curves in (**b**) corresponds to $\gamma = -1$ (on-site *solid line*, intersite *solid line with circles*), $\gamma = -3$ (on-site *dashed line*, intersite *dashed line with squares*), and $\gamma = -5$ (on-site *dotted line*, intersite *dotted line with triangles*), respectively
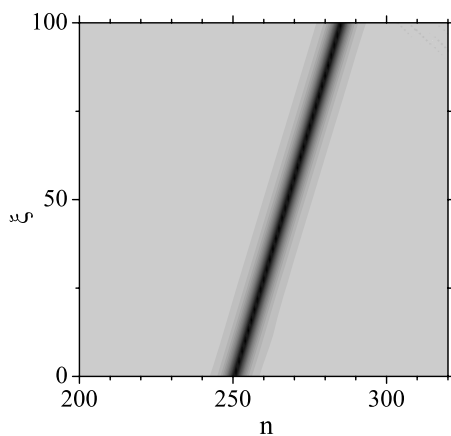
Fig. 5 Free steering of on-site dark unstaggered soliton with $\gamma = -3$, $P = 4.42$, and $\mu = 3.15$ which is transversely kicked ($u_n \exp(ikn)$). Here $\phi = \pi/18$

solitons, see Fig. 3c, breathers [31], or diffract, see Fig. 3d. Actually the evolution is determined by the closeness to the stable branch in the sense that if a stable dark counterpart exists the unstable mode evolves to the corresponding breather ([16, 27] and references therein).

5 Mobility issues

One important feature of lattice solitons is the existence of an effective periodic potential which affects free steering of solitons through the NWA. This potential is investigated in the context of dislocation theory by Peierls and Nabarro [32, 33] and originates from the broken translational symmetry. The concept of the Peierls–Nabarro (PN) barrier [12, 22, 34, 35] found its application in determining whether or not it is possible to find mobile modes in transversal direction of a discrete system, which is quite important for information transport. The PN barrier is equal to the difference of the corresponding Hamiltonians (or free energies) of

on-site and intersite solitons with the same power. Briefly, mobile solitons exist only in those regions in which this barrier tends to zero. In this article, we follow procedures which have been used in [12] and [16].

Figure 4a depicts the dependence of free energy G on soliton power P ($G = H - \omega P$) for $\gamma = 1$ for bright gap modes. Obviously, a considerable PN barrier exists and we confirm this result for many different values of parameter γ. Thus, gap solitons are immobile, i.e., they are always pinned to the predefined channel of the NWA.

Free energy and all conserved quantities of dark modes have to be normalized with respect to the plane-wave background in order to avoid divergence. We present the dependence of complementary free energy G_c on complementary power $P_c = P - U_0^2$ and complementary Hamiltonian $H_c = H + \gamma P_c/(1 - U_0^2) - \gamma N \ln(1 - U_0^2)$): $G_c = H_c - \omega P_c$ (U_0 is the background amplitude and N is the total number of lattice elements) for different values of the nonlinear coefficient in Fig. 4b. For each specific value of parameter γ it is possible to find fundamental modes whose PN barrier vanishes. In these power regions the separation between the $G_c(P_c)$ curves for on-site and intersite solitons (Fig. 4b) and separation between the $P_c(\omega)$ curves for on-site and intersite solitons (Fig. 1b) simultaneously vanishes. One example of free steering of an unstaggered on-site dark soliton is shown in Fig. 5.

6 Conclusions

We have studied theoretically optical-wave propagation in one-dimensional periodic media possessing an intensity-resonant nonlinearity. Regions of stability and existence of various stationary solutions, including gap and dark solitons, have been identified. We prove that, within the model, it is possible to find system parameters to have at least marginally stable propagation of both fundamental gap and

dark modes. An omnipresent Peierls–Nabarro barrier disables free steering of gap solitons but may disappear in the case of unstaggered dark solitons. All results are checked numerically. In the future, it would be interesting to fabricate permanent NWAs in InP:Fe and explore beam interactions and features of other more complex types of localized modes, which may enable soliton-based light–light interactions in periodic media with fast response times in the microsecond regime.

References

1. M. Segev, B. Crosignani, A. Yariv, B. Fischer, Phys. Rev. Lett. **68**, 923 (1992)
2. G.C. Duree, J.L. Shultz, G.J. Salamo, M. Segev, A. Yariv, B. Crosignani, P. Di Porto, E.J. Sharp, R.R. Neurgaonkar, Phys. Rev. Lett. **71**, 533 (1993)
3. M.D. Iturbe-Castillo, P.A. Marquez-Aguilar, J.J. Sanchez-Mondragon, S. Stepanov, V. Vysloukh et al., Appl. Phys. Lett. **64**, 408 (1994)
4. G.C. Valley, M. Segev, B. Crosignani, A. Yariv, M.M. Fejer, M.C. Bashaw, Phys. Rev. A **50**, R4457 (1994)
5. J.W. Fleischer, G. Bartel, O. Cohen, T. Schwartz, O. Manela, B. Freedman, M. Segev, H. Buljan, N.K. Efremidis, Opt. Express **13**, 1780 (2005)
6. J.W. Fleischer, T. Carmon, M. Segev, N.K. Efremidis, D.N. Christodoulides, Phys. Rev. Lett. **90**, 023902 (2003)
7. F. Chen, M. Stepić, C.E. Rüter, D. Runde, D. Kip, V. Shandarov, O. Manela, M. Segev, Opt. Express **13**, 4314 (2005)
8. B. Mainguet, Opt. Lett. **13**, 657 (1988)
9. G. Picoli, P. Gravey, C. Ozkul, V. Vieux, J. Appl. Phys. **66**, 3798 (1989)
10. M. Chauvet, S.A. Hawkins, G.J. Salamo, M. Segev, D.F. Bliss, G. Bryant, Opt. Lett. **21**, 1333 (1996)
11. R. Uzdin, M. Segev, G.J. Salamo, Opt. Lett. **26**, 1547 (2001)
12. M. Stepić, A. Maluckov, M. Stojanović, F. Chen, D. Kip, Phys. Rev. A **78**, 043819 (2008)
13. D.N. Christodoulides, R.I. Joseph, Opt. Lett. **13**, 794 (1988)
14. Yu.S. Kivshar, Opt. Lett. **18**, 1147 (1993)
15. D.N. Christodoulides, M.I. Carvalho, J. Opt. Soc. Am. B **12**, 1628 (1995)
16. Lj. Hadžievski, A. Maluckov, M. Stepić, Opt. Express **15**, 5687 (2007)
17. W. Chen, D.L. Mills, Phys. Rev. Lett. **58**, 160 (1987)
18. J.E. Sipe, H.G. Winful, Opt. Lett. **13**, 132 (1988)
19. D. Mandelik, R. Morandotti, J.S. Aitchison, Y. Silberberg, Phys. Rev. Lett. **92**, 093904 (2004)
20. A. Hasegawa, F. Tappert, Appl. Phys. Lett. **23**, 171 (1973)
21. S. Burger, K. Bongs, S. Dettmer, W. Ertmer, K. Sengstock, A. Sanpera, G.V. Shlyapnikov, M. Lewenstein, Phys. Rev. Lett. **83**, 5198 (1999)
22. Yu.S. Kivshar, W. Królikowski, O.A. Chubykalo, Phys. Rev. E **50**, 5020 (1994)
23. J. Meier, G.I. Stegeman, D.N. Christodoulides, Y. Silberberg, R. Morandotti, H. Yang, G. Salamo, M. Sorel, J.S. Aitchison, Phys. Rev. Lett. **92**, 163902 (2004)
24. M. Stepić, C. Wirth, C.E. Rüter, D. Kip, Opt. Lett. **31**, 247 (2006)
25. A. De Rossi, C. Conti, S. Trillo, Phys. Rev. Lett. **81**, 85 (1998)
26. I.V. Barashenkov, D.E. Pelinovsky, E.V. Zemlyanaya, Phys. Rev. Lett. **80**, 5117 (1998)
27. A. Maluckov, Lj. Hadžievski, B.A. Malomed, Phys. Rev. E **76**, 046605 (2007)
28. I.V. Barashenkov, Phys. Rev. Lett. **77**, 1193 (1996)
29. E. Smirnov, C.E. Rüter, M. Stepić, D. Kip, V. Shandarov, Phys. Rev. E **74**, 065601(R) (2006)
30. D.E. Pelinovsky, P.G. Kevrekidis, J. Phys. A **41**, 182506 (2008)
31. S. Flach, A.V. Gorbach, Phys. Rep. **467**, 1 (2008)
32. R.F. Peierls, Proc. R. Soc. Lond. **52**, 34 (1940)
33. F.R.N. Nabarro, Proc. R. Soc. Lond. **59**, 256 (1947)
34. Yu.S. Kivshar, D.K. Campbell, Phys. Rev. E **48**, 3077 (1993)
35. Lj. Hadžievski, A. Maluckov, M. Stepić, D. Kip, Phys. Rev. Lett. **93**, 033901 (2004)